batteries

MDPI

Article

Sustainable Recovery of Critical Metals from Spent Lithium-Ion Batteries Using Deep Eutectic Solvents

Jafar Goudarzi [1], Zhi Chen [1,2,*], Gaixia Zhang [3], Jinguang Hu [4], Karim Zaghib [5], Sixu Deng [5], Afzal Ahmed Dar [1], Xiaolei Wang [6], Fariborz Haghighat [1,2], Catherine N. Mulligan [1,2], Chunjiang An [1,2] and Antonio Avalos Ramirez [7]

1 Department of Building, Civil, and Environmental Engineering, Concordia University, 1455 de Maisonneuve Blvd. W., Montreal, QC H3G 1M8, Canada; jafar.goudarzi@mail.concordia.ca (J.G.); afzalahmed.dar@concordia.ca (A.A.D.); fariborz.haghighat@concordia.ca (F.H.); mulligan@civil.concordia.ca (C.N.M.); chunjiang.an@concordia.ca (C.A.)

2 Concordia Institute of Water, Energy and Sustainable Systems, Concordia University, Montreal, QC H3G 1M8, Canada

3 Department of Electrical Engineering, École de Technologie Supérieure (ÉTS), Montreal, QC H3C 1K3, Canada; gaixia.zhang@etsmtl.ca

4 Department of Chemical and Petroleum Engineering, University of Calgary, 2500 University Drive, NW, Calgary, AB T2N 1N4, Canada; jinguang.hu@ucalgary.ca

5 Department of Chemical and Materials Engineering, Concordia University, 1455 de Maisonneuve Blvd. W., Montreal, QC H3G 1M8, Canada; karim.zaghib@concordia.ca (K.Z.); sixu.deng@concordia.ca (S.D.)

6 Department of Chemical and Materials Engineering, University of Alberta, 12-241 Donadeo Innovation Centre for Engineering, 9211-116 Street NW, Edmonton, AB T6G 1H9, Canada; xiaolei.wang@ualberta.ca

7 Centre National en Électrochimie et en Technologies Environnementales, 2263 Av. du Collège, Shawinigan, QC G9N 6V8, Canada; aaramirez@cnete.qc.ca

* Correspondence: zhi.chen@concordia.ca

Abstract

The surging demand for lithium-ion batteries (LIBs) has intensified the need for sustainable recovery of critical metals such as lithium, manganese, cobalt, and nickel from spent cathodes. While conventional hydrometallurgical and pyrometallurgical methods are widely used, they involve high energy consumption, hazardous waste generation, and complex processing steps, underscoring the urgency of developing eco-friendly alternatives. This study presents a novel, water-enhanced deep eutectic solvent (DES) system composed of choline chloride and D-glucose for the efficient leaching of valuable metals from spent LiMn-based battery cathodes. The DES was synthesized under mild conditions and applied to dissolve cathode powder, with leaching performance optimized by varying temperature and duration. Under optimal conditions (100 °C, 24 h), exceptional recovery efficiencies were achieved: 98.9% for lithium, 98.4% for manganese, and 71.7% for nickel. Material characterization using X-ray diffraction (XRD), Fourier-transform infrared spectroscopy (FTIR), differential scanning calorimetry (DSC), and inductively coupled plasma mass spectrometer (ICP-MS) confirm effective phase dissolution and metal release. Although this DES system requires relatively higher temperature and longer reaction time compared to traditional acid leaching, it offers clear advantages in terms of non-toxicity, biodegradability, and elimination of strong oxidizing agents. These results demonstrate the potential of water-enhanced choline chloride–glucose DES as a green alternative for future development in sustainable battery recycling, supporting circular economy objectives.

Keywords: lithium-ion battery; recycling; deep eutectic solvent; D-glucose; choline chloride; leaching; hydrogen bonding network

check for updates

Academic Editor: Yong-Joon Park

Received: 16 July 2025

Revised: 15 August 2025

Accepted: 11 September 2025

Published: 14 September 2025

Citation: Goudarzi, J.; Chen, Z.; Zhang, G.; Hu, J.; Zaghib, K.; Deng, S.; Dar, A.A.; Wang, X.; Haghighat, F.; Mulligan, C.N.; et al. Sustainable Recovery of Critical Metals from Spent Lithium-Ion Batteries Using Deep Eutectic Solvents. *Batteries* **2025**, *11*, 340. https://doi.org/10.3390/batteries11090340

1. Introduction

Over the past decade, LIBs have become indispensable in modern technology due to their widespread application in portable electronics, electric vehicles (EVs), and grid-scale renewable energy storage systems [1–4]. Their superior energy density, lightweight design, and high charge–discharge efficiency have positioned LIBs as a cornerstone of clean energy transitions. However, the rising demand for LIBs raises environmental and economic concerns, particularly at their end-of-life (EoL) stage [2–10].

A typical LIB is composed of several key components: a cathode, anode, separator, electrolyte, and polymer binder [11,12]. Among these, the cathode is the most valuable and resource-intensive component, contributing approximately 40–50% of the total battery manufacturing cost [13,14]. Typical chemistries include lithium cobalt oxide (LCO), lithium manganese oxide (LMO), lithium iron phosphate (LFP), nickel–manganese–cobalt oxide (NMC), and nickel–cobalt–aluminum oxide (NCA), each offering specific advantages [11,13,15,16]. These active materials are coated on aluminum foil using a polyvinylidene fluoride (PVDF) binder, while graphite anodes are typically adhered to copper foil. Consequently, spent LIBs are rich in recoverable metals such as Li, Co, Ni, Mn, Al, and Cu [7,17–20].

Recycling of LIBs is vital for environmental protection and resource conservation. Currently, pyrometallurgy and hydrometallurgy are the dominant recycling methods. Pyrometallurgy employs high temperatures for smelting and reduction, enabling recovery of valuable metals but at the cost of significant energy consumption and emission of toxic gases [21–25]. Hydrometallurgy dissolves metals into solutions using strong inorganic acids such as sulfuric or nitric acid, providing higher selectivity and recovery rates but resulting in corrosive wastewater and secondary pollution [26–28]. Although organic acids like citric, oxalic, and ascorbic acids have been explored as greener alternatives, they often require additional steps—such as the use of reducing agents or ultrasound—to achieve effective metal recovery, which can increase costs [29–32].

In recent years, deep eutectic solvents (DESs) have gained attention as promising alternatives due to their green chemistry profile. Formed by mixing a hydrogen bond acceptor (HBA) and hydrogen bond donor (HBD), DESs are biodegradable, exhibit low toxicity, and possess negligible vapor pressure [33–36]. Choline chloride (ChCl), a common HBA, is often paired with HBDs like urea, ethylene glycol, or carboxylic acids to form effective metal-leaching systems [1,14,37]. Among them, D-glucose stands out as a naturally abundant, biodegradable sugar that offers multiple hydroxyl groups for hydrogen bonding, making it an excellent and underexplored HBD for DES-based leaching applications. This study leverages ChCl and D-glucose to formulate a novel eutectic mixture, aimed at enhancing both metal dissolution and system sustainability. The leaching mechanism typically involves metal–ligand complexation and redox reactions, facilitated by the DES's acidity and coordination ability, while its inherently higher viscosity compared to aqueous solutions can impede mass transfer unless mitigated by dilution or co-solvent addition [38–40].

Ebrahimi et al. (2023) [17] demonstrated that a ternary DES system could recover metals from NMC cathodes at 100 °C within 72 h, illustrating the potential of DESs to compete with traditional hydrometallurgical processes under milder conditions. However, high viscosity remains a critical challenge, especially when processing complex residues like black mass. Strategies such as increasing temperature or adding reducing agents can improve leaching performance but may offset DESs' environmental advantages by increasing energy consumption and operational costs [41].

Despite their promise, DESs still face challenges for industrial-scale implementation. One of the main obstacles is high viscosity, which reduces mass transfer efficiency and often requires the addition of co-solvents like dimethyl sulfoxide (DMSO) or elevated temperatures to improve leaching kinetics [41]. Moreover, many studies focus on pure cathode powders or pre-treated samples, whereas real spent batteries often yield a complex residue known as black mass (BM)—a heterogeneous mixture containing active materials, binders, carbon black, residual electrolyte, and Al/Cu foil particles [5,42,43]. Efficient recovery from BM requires DES systems that can overcome interference from these impurities while maintaining high selectivity for valuable metals.

Recent reviews have highlighted the potential of DESs in solvometallurgical recycling pathways that bridge the benefits of hydrometallurgy and solvent extraction [44]. These approaches reduce reliance on strong acids and minimize secondary waste generation. However, they require further optimization in terms of leaching time, temperature, solid-to-liquid ratio, and reagent regeneration. Moreover, the mechanism of metal complexation and precipitation from DES leachates remains an area of active investigation [14].

This study aims to develop and evaluate a deep eutectic solvent (DES) based on choline chloride and D-glucose as a potentially greener and effective medium for the recovery of critical metals, e.g., lithium, manganese, and nickel, from spent lithium-ion batteries. While the preparation and sourcing of choline chloride entail certain economic and environmental costs, the DES system investigated here offers operational advantages compared to conventional mineral acid leaching, including lower volatility, reduced corrosivity, and potential for solvent reuse. The primary objective is to explore the potential of this DES system to achieve high metal leaching efficiencies under mild operational conditions, such as lower temperatures and shorter reaction times, thereby reducing environmental and energy-related impacts. A further objective is to investigate the role of D-glucose as the hydrogen bond donor in enhancing leaching performance through improved hydrogen bonding and metal complexation. Additionally, the study seeks to address the challenge of high viscosity inherent to DESs by incorporating water into the formulation, with the goal of improving mass transfer, reducing energy input, and accelerating leaching kinetics while maintaining the overall environmental advantages of the solvent system.

2. Materials and Experimental

2.1. Materials

Spent lithium-ion batteries (LIBs) were used as the primary source of cathode material in this study. Specifically, MNKE IMR 18650 30A cells (model MH4669, MNKE Battery, Jiangsu Eastdye Battery Co., Ltd., Changzhou, Jiangsu, China) were selected. According to the manufacturer, these cells employ an LMO-type ($LiMn_2O_4$) spinel cathode. Consistent with this, our XRD identifies a $LiMn_2O_4$-type spinel with partial Ni/Co substitution, i.e., Li $(Mn,Ni,Co)_2O_4$, together with minor CoO. To recover the active cathode powder, the cells were dismantled, and the aluminum current collector was removed by immersing the cathode in a 7 M sodium hydroxide (NaOH) solution. The extracted powder was then subjected to acid digestion using a mixture of concentrated hydrochloric acid (HCl) and nitric acid (HNO_3) to prepare the leachate for elemental analysis via inductively coupled plasma (ICP).

Deep eutectic solvent (DES) was synthesized using choline chloride (ChCl) and D-glucose. All chemicals, including NaOH, HCl, H_2SO_4, ChCl, and D-glucose, were purchased from Thermo Fisher Scientific (Waltham, MA, USA). Deionized (DI) water, obtained from an in-lab water purification system, was used for all experimental procedures, including sample preparation, washing, and dilution.

2.2. Instrumentation and Analysis Methods

A comprehensive set of analytical techniques was employed to characterize the materials and assess the efficiency of the leaching process. Inductively Coupled Plasma Mass Spectrometer (ICP-MS, 7700 series, Agilent, Santa Clara, CA, USA) was used to determine the concentration of metal ions in the cathode material. Additionally, an Atomic Absorption Spectrometer (AAS, PerkinElmer, Waltham, MA, USA) was utilized to measure metal concentrations during the leaching process, enabling the calculation of leaching efficiency.

The characterization of the DES and its components was conducted using Fourier Transform Infrared Spectroscopy (FTIR, PerkinElmer, Waltham, MA, USA), while Differential Scanning Calorimetry (DSC, TA Universal, New Castle, DE, USA) was employed to investigate the thermal behavior and confirm DES formation.

The structural properties of the cathode material were analyzed using X-ray Diffraction (XRD, Rigaku, Tokyo, Japan). Particle size distribution was determined with a HORIBA Laser Scattering Particle Size Distribution Analyzer (LA-960, HORIBA Scientific, Kyoto, Japan). Additionally, a ball milling machine (Retsch, PM 200, Haan, Germany) was used to grind the cathode material with the aim of achieving a particle size below 75 μm for further processing.

2.3. Methodology

Spent LIBs were collected from the waste storage at Concordia University, Montreal, Canada. To mitigate the risk of fire during disassembly, the batteries were submerged in a 10% sodium chloride solution for 48 h to reduce their voltage to below 2 V, ensuring safe handling before the dismantling process [45,46]. The spent LIBs were manually disassembled using standard tools such as pliers and blades, to isolate the active cathode materials [47]. To minimize contamination, non-cathode components, including steel casings, anode sections, and plastic parts, were carefully removed. The cathode material, still adhered to aluminum foil, was then treated with a 7 M NaOH solution to selectively dissolve the aluminum according to the reaction:

$$Al + 2NaOH + 2H_2O \rightarrow 2NaAlO_2 + 3H_2 \quad (1)$$

After the aluminum dissolution, the remaining cathode material was separated via filtration and thoroughly washed to eliminate any residual solution. To remove organic binders such as polyvinylidene fluoride (PVDF) and conductive additives like carbon black, the material was dried at 70 °C for 24 h. Subsequently, the spent cathode material underwent calcination at 600 °C for 6 h to eliminate residual graphite and other impurities. Finally, the purified cathode material was finely milled using a ball milling machine to reduce particle size and increase surface area for further processing [46,47]. The particle size distribution of the cathode powder was measured using a Laser Scattering Particle Size Distribution Analyzer (Horiba LA-960, HORIBA Scientific, Kyoto, Japan). The analysis was performed under agitation speed setting 3, with ultrasonic dispersion applied for 20 s to ensure homogenous dispersion. A refractive index of 1.44–0.10i was used. The output included frequency and cumulative distributions, as well as statistical values such as mean, median, and standard deviation. To analyze the metal content of the cathode powder, 0.5 g of the dried sample was weighed and dissolved in 20 mL of an acid mixture consisting of concentrated nitric acid (HNO_3, 65%) and hydrochloric acid (HCl, 36%) in a 1:3 (v/v) ratio. The mixture was digested for 1.5 h at room temperature. After digestion, 15 mL of the solution was transferred to a 100 mL volumetric flask and diluted to the mark with demineralized water. From this solution, 1 mL was taken and further diluted to 25 mL using 1% HNO_3 to prepare the final sample for ICP analysis.

2.3.1. Preparation for DES

Two types of deep eutectic solvents (DESs) were prepared: binary DES and ternary DES, both utilizing choline chloride (ChCl) ([$(CH_3)_3NCH_2CH_2OH$] Cl) as the hydrogen bond acceptor. For the binary DES, choline chloride and dextrose (D-glucose) ($C_6H_{12}O_6$) were mixed in a 2:1 molar ratio and heated at 70 °C with continuous stirring at 400 rpm for 3 h until a homogeneous and transparent liquid was formed [46,48]. However, the binary DES exhibited excessively high viscosity, making handling difficult and potentially limiting metal ion diffusion during the leaching process.

To reduce viscosity and enhance leaching efficiency, a ternary DES was formulated by incorporating 10 wt.% water into the ChCl-D-glucose system. The primary advantage of the ternary DES lies in its enhanced leaching performance due to improved fluidity and mass transfer, rather than simply reducing the preparation time or mixing energy. This modification reduced the formation time, as the ternary DES was obtained within 30 min under the same temperature (70 °C) and stirring speed (400 rpm). The addition of water improved fluidity while maintaining solvent stability [48]. Both DES formulations were stored in sealed containers at room temperature and used for subsequent leaching experiments.

2.3.2. Leaching Process

A specific amount of cathode powder (50 mg) was added to 5 mL of the produced DES in a glass vial. Due to sample availability and instrument access limitations, each leaching condition was tested once as a representative measurement. The results are intended to indicate the general trends observed under the tested conditions. To examine their impact on metal leaching and extraction, the mixture was stirred at 400 rpm on a hotplate stirrer under various temperature and time conditions. Temperatures between 60 and 110 °C and extraction durations between 2 and 24 h were among the parameters under investigation. Following the extraction procedure, each sample was filtered using a 0.45 μm syringe filter, and the filtrate was then analyzed by atomic absorption spectroscopy (AAS) to determine the concentrations of dissolved metals. The following equation was used to calculate the metal extraction efficiency (η):

$$\eta = (C_{Me} \times V)/(m \times X) \times 100 \quad (2)$$

where C_{Me} is the metal ion concentration of Li, Co, Ni, and Mn ($mg \cdot L^{-1}$); V is the volume of the leaching solution (L); m is the mass of the NCM powder (cathode active material, mg); and X is the mass fraction of Li, Co, Ni, and Mn in the cathode active material.

Each leaching condition was performed once as a single batch due to sample and instrument constraints. For analytical reliability, metal concentrations in each filtrate were measured in triplicate (three aliquots of the same solution) by AAS, and the mean value is reported. These are instrumental/analytical replicates, not independent experimental replicates. Consequently, error bars representing experimental variability are not shown, and the results are intended to indicate the observed trends under the tested conditions.

3. Results and Discussion

3.1. Characterizations of the Spent LIB Sample and DES

The particle size distribution of the cathode powder is presented in Figure 1. The red frequency distribution curve indicates that most particles fall within the clay-size range. The green cumulative curve shows that approximately 90% of the particles are smaller than 3 μm, with a sharp rise suggesting a uniform and fine particle distribution. The measured median particle size was 1.513 μm, and the mean size was 1.802 μm, with a standard deviation of 1.093 μm.

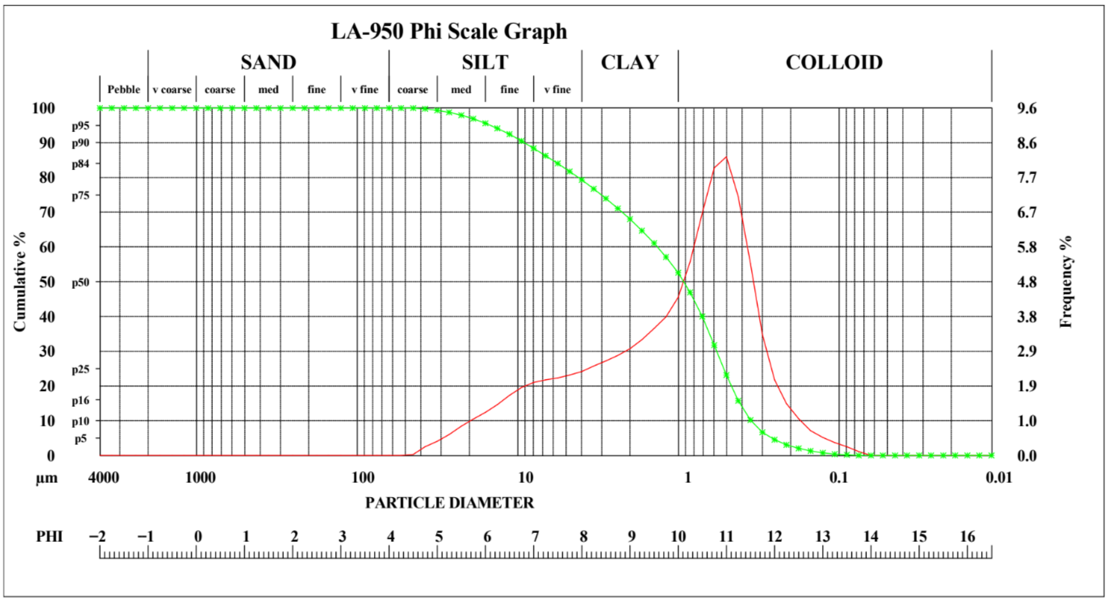

Figure 1. Results of particle size distribution analysis for the ball-milled cathode powder obtained using the LA-950 analyzer. The green line represents the cumulative particle size distribution (%), while the red line indicates the frequency distribution (%).

After the acid digestion process, an ICP (Inductively Coupled Plasma) analysis was performed to measure the concentrations of various metals in the cathode powder. As shown in Table 1. Elemental composition of cathode powder analyzed by ICP, very small trace amounts of aluminum and copper were detected in the powder. This indicates that the aluminum removal and impurity elimination processes, carried out through dissolution in sodium hydroxide, were effectively executed. The low presence of these metals (0.17 wt.% Al and 0.017 wt.% Cu) suggests that the purification process was successful, leading to a relatively clean cathode material suitable for further analysis and recovery processes. The use of ICP-MS was crucial in accurately characterizing the metal composition of the cathode powder.

Table 1. Elemental composition of cathode powder analyzed by ICP-MS.

Element	Lithium (Li)	Manganese (Mn)	Nickel (Ni)	Cobalt (Co)	Aluminum (Al)	Copper (Cu)
Weight Percentage (%)	2.5	33.78	8.74	7.90	0.17	0.017

In this study we focus on introducing a water-enhanced choline chloride–D-glucose DES that lowers viscosity and melting point, accelerating mass transfer and enabling greener leaching of Li-ion cathodes. It is expected that this environmentally friendly, non-toxic, and biodegradable alternative also offers tunable metal selectivity via DES composition. Li, Mn, and Ni will be examined using the enhanced DES based on prioritization. Building on the results, we will next apply the same DES platform to cobalt and other precious metals.

The X-ray diffraction (XRD) pattern of the cathode material after heat treatment at 600 °C for 6 h (Figure 2) is dominated by reflections characteristic of a spinel Li $(Mn,Ni,Co)_2O_4$ structure, confirming partial substitution of Mn by Ni and Co as indicated by the elemental composition in Table 1. The primary diffraction peaks at $2\theta \approx 18.7°$ (111), 36.3° (311), 44.2° (400), 58.3° (511), and 64.0° (440) correspond well to the $LiMn_2O_4$-

type spinel phase (ICDD PDF 35-0782). The pronounced (111) reflection indicates high crystallinity, while the close match of other reflections shows that the overall spinel framework is preserved. The slight shifts in peak positions are consistent with lattice distortion caused by Ni/Co substitution at Mn sites. In addition to the Li-containing spinel phase, weak reflections near ~42.4° and ~73.7° match those expected for a minor CoO phase. Furthermore, weak peaks near ~18.9° and ~44.5° may coincide with $LiCoO_2$ (003, 104) reflections, but their low intensity and the compositional data suggest $LiCoO_2$ is a minor or impurity phase rather than a primary constituent.

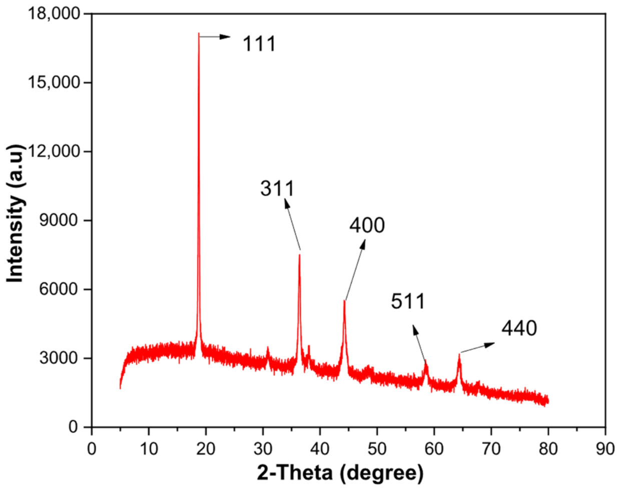

Figure 2. XRD pattern of the active cathode material after heat treatment at 600 °C for 6 h. Major peaks are indexed as (hkl) and correspond to the spinel Li $(Mn,Ni,Co)_2O_4$ phase; weak features are consistent with minor CoO (e.g., weak features near ~42.4° and ~73.7° are consistent with CoO).

The Differential Scanning Calorimetry (DSC) analysis confirms the successful formation of deep eutectic solvents (DESs) through a significant reduction in melting points compared to their individual components (Figure 3). The binary DES (ChCl + D-glucose) exhibits a melting point of 81.06 °C, while the ternary DES (ChCl + D-glucose + 10 wt.% water) melts at 50.34 °C. This decreases in melting temperature, relative to pure choline chloride (302 °C) and D-glucose (146 °C), confirms eutectic formation. While strong hydrogen bonding between ChCl and glucose can restrict molecular mobility and thus raise the melting point, the incorporation of water disrupts these interactions, lowering the melting temperature. The very small molecular size of water, compared to ChCl and glucose, likely further enhances the entropy of mixing and stabilizes the liquid phase at lower temperatures [33,49].

The addition of 10 wt.% water in the ternary DES significantly influences its thermal properties. Water acts as a hydrogen bond donor and plasticizer, weakening intermolecular interactions and further lowering the melting point [50–53]. This effect is well-documented in previous studies, where water incorporation enhances fluidity, reduces viscosity, and expands the liquid phase stability of DESs [53,54]. The lower melting point of the ternary DES compared to the binary system highlights the critical role of water in modifying the physicochemical properties of eutectic solvents, making them more adaptable for various applications.

In addition to the shift in melting points, the DSC thermograms reveal a distinct difference in peak shapes between the binary and ternary DESs. The binary DES shows a sharp, well-defined endothermic peak, indicating a relatively ordered hydrogen bonding network and a clear phase transition. In contrast, the ternary DES exhibits a broader and smoother melting peak. This can be attributed to the structural disruption caused by the presence of water, which introduces molecular disorder and increases configurational entropy. Water interferes with the organized hydrogen bonding between ChCl and glucose, resulting in a distribution of melting events over a broader temperature range. Similar broad thermal transitions in water-containing DESs have been reported in previous studies [49], supporting the view that the broadened peak reflects increased heterogeneity in the system.

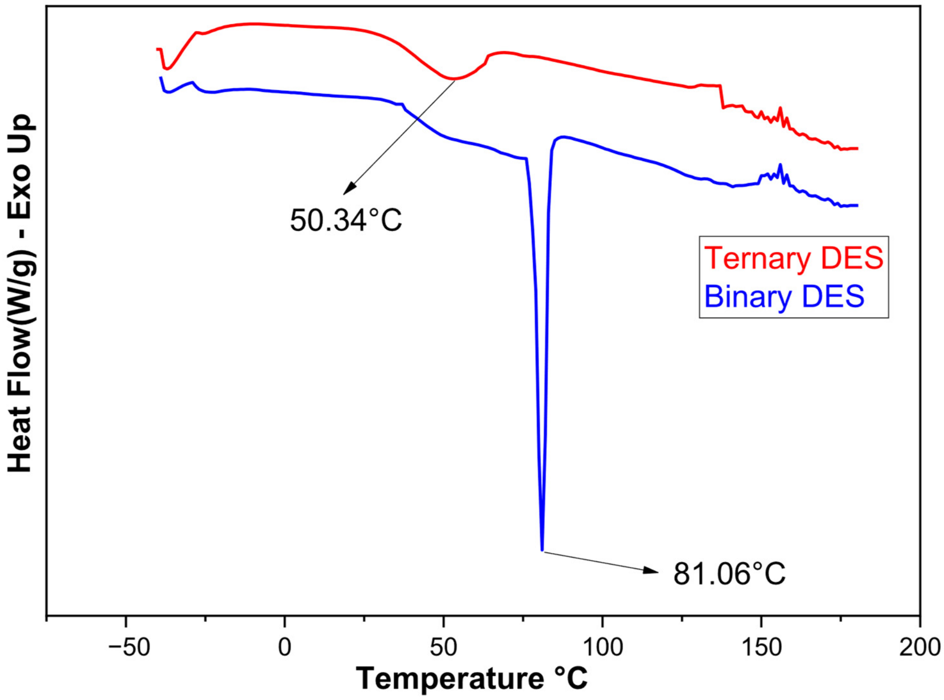

Figure 3. The DSC of the ternary and binary DES from −50 °C to 180 °C.

Figure 4 illustrates the viscosity behavior of binary and ternary DES systems evaluated at room temperature (25 °C) across various spindle speeds ranging from 50 to 500 RPM. The binary DES, composed of choline chloride and glucose, exhibited significantly higher viscosities, starting at 6.6 Pa·s at 50 RPM and gradually decreasing to 5.31 Pa·s at 500 RPM. In contrast, the ternary DES—prepared by incorporating 10 wt.% water—showed a much lower viscosity range, from 2.1 Pa·s to 1.065 Pa·s. The consistent decrease in viscosity with increasing speed indicates pseudoplastic (shear-thinning) behavior, which is typical of DES systems. The considerable reduction in viscosity upon water addition is attributed to the disruption of the strong hydrogen bonding network between DES components. This not only reduces internal resistance and improves fluidity, but also enhances mass transport and diffusion [48,51,55]. Such improved dynamic properties are particularly beneficial in leaching applications, where efficient metal recovery from spent batteries depends heavily on effective solvent mobility.

Figure 5 presents the UV-Vis absorption spectra of both binary and ternary DES systems, as well as a reference blank, over the wavelength range of 200 to 350 nm. The binary DES (Choline Chloride: Glucose) and the ternary DES (with 10 wt.% water added) exhibit remarkably similar spectral profiles, with a strong absorbance peak below 220 nm followed by a rapid decline toward baseline levels above 250 nm. The pronounced absorption in the deep UV region (<220 nm) is attributed to the $n \rightarrow \sigma^*$ and $\pi \rightarrow \pi^*$ electronic transitions associated with functional groups such as hydroxyls and amines, which are abundant in both DES constituents. The similarity between the two spectra suggests that the addition of 10 wt.% water does not significantly alter the electronic environment or the primary functional group interactions within the DES system. This implies that while water affects physical properties like viscosity, it does not disrupt the core molecular structure or bonding configurations responsible for UV absorbance. Therefore, comparable spectral behavior supports the chemical stability of the DES system upon water incorporation, which is favorable for maintaining leaching functionality during hydrometallurgical processing.

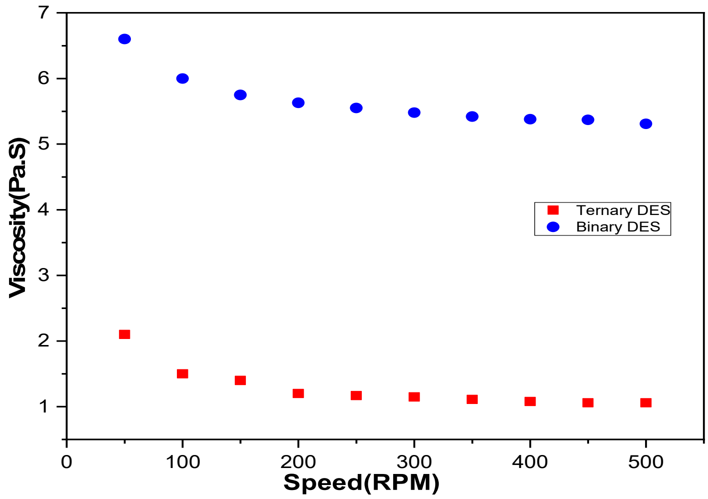

Figure 4. Viscosity comparison of binary and ternary DESs at room temperature.

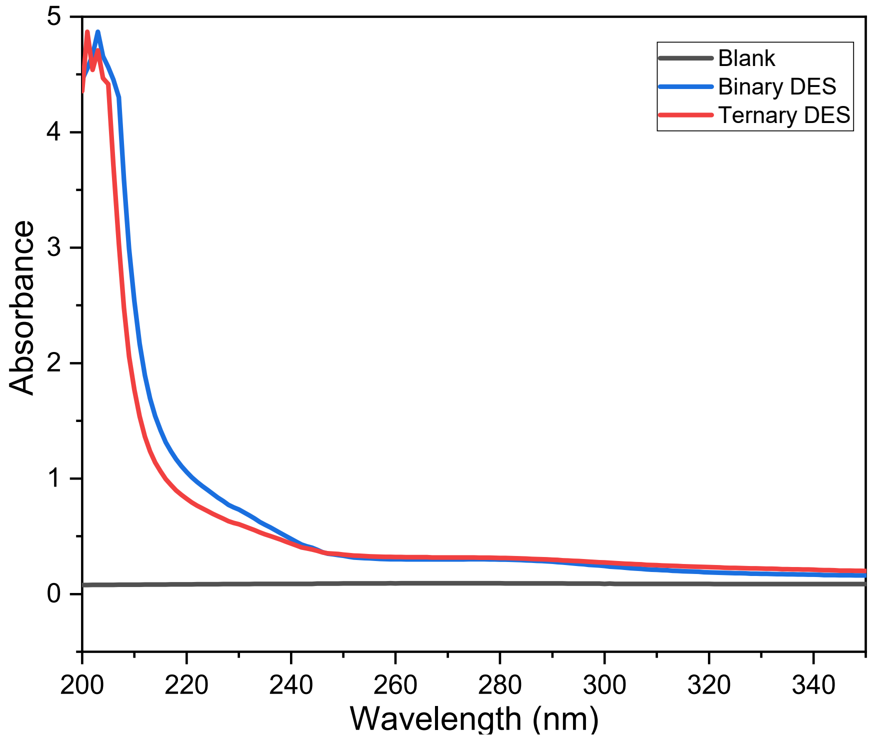

Figure 5. UV-Vis spectra of binary and ternary DESs between 200 and 400 nm.

The FTIR spectra (Figure 6) confirms formation of the DES (ChCl + D-glucose + water) through shifts in key vibrational bands. The broad O–H stretching band, observed at ~3220 cm^{-1} (ChCl) and ~3198 cm^{-1} (D-glucose), shifts to ~3265 cm^{-1} in the DES, indicating a modified (weaker) hydrogen-bonding network. A C–H stretching band appears at ~2922 cm^{-1} in the DES. The glucose C–O stretching band shifts from ~990 to ~1028 cm^{-1} in the DES, consistent with hydrogen-bond-affected bond environments. A band near ~1471 cm^{-1} is assigned to C–H scissoring, and the ~954 cm^{-1} band associated with the quaternary ammonium of ChCl remains, indicating retention of ionic character. Taken together, these features confirm DES formation with an overall weaker hydrogen-bonding network, consistent with the DSC evidence that added water disrupts strong interactions and lowers the melting point.

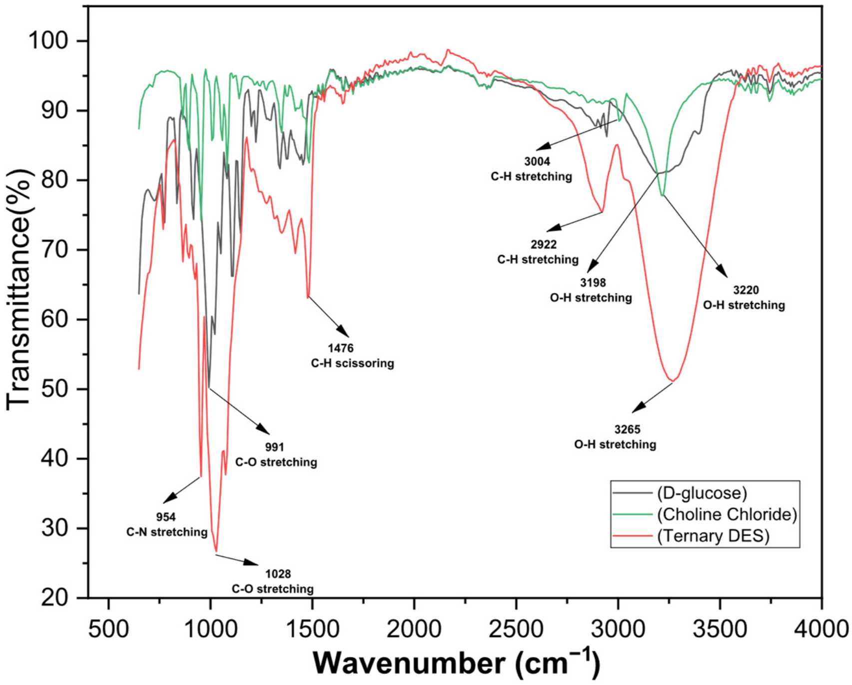

Figure 6. FTIR spectra comparing the DES with its individual components (choline chloride and glucose).

3.2. Leaching of Spent LIB Sample

3.2.1. Effect of Temperature on Leaching Efficiency Using Binary and Ternary DES

The leaching experiments were conducted at various temperatures with a fixed leaching time of 24 h. Figures 7 and 8 present the comparative leaching efficiency of Li, Mn, and Ni at different temperatures (60–110 °C) using binary and ternary deep eutectic solvents (DESs). The results show that the ternary DES system exhibits significantly higher leaching efficiencies for all three metals across the tested temperature range compared to the binary DES system.

In the case of the binary DES system (Figure 8), the leaching efficiencies of Li, Mn, and Ni increased with temperature, reaching maximum values of 88.1%, 84.2%, and 54.8% at 110 °C, respectively. Although the melting point of the binary ChCl–glucose DES is approximately 81 °C (as confirmed by DSC analysis), leaching tests were also conducted at 60 °C to assess the threshold of leaching performance. At this lower temperature, the DES exists in a semi-solid or highly viscous state, but partial liquefaction and limited molecular mobility occur under continuous heating and stirring, permitting partial metal leaching with reduced efficiency. These results illustrate the onset of leaching capability below the melting point and support the identification of 100 °C as the optimal temperature for efficient metal extraction with this DES system. At lower temperatures (e.g., 60 °C), extraction efficiencies were substantially lower, particularly for Ni (7.6%) likely due to the stronger crystal-field stabilization and ionic bonding of Ni within the host spinel lattice (with Ni/Co substitution). Similar trends have been reported in previous studies, where Ni exhibited lower leaching rates because of its higher lattice energy and lower mobility compared to Li and Mn [30,56]. The consistent improvement in Li and Mn leaching with increasing temperature aligns with kinetic models indicating that higher temperatures enhance diffusion and surface reaction rates in DES systems.

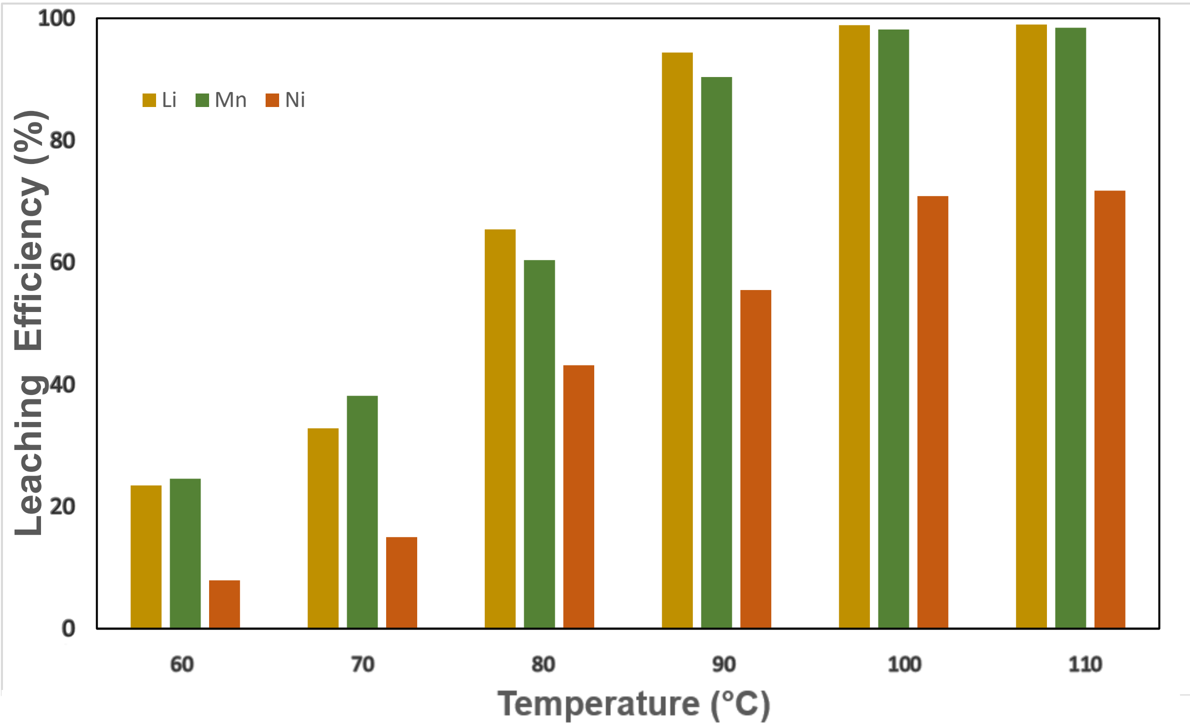

Figure 7. Effect of temperature on leaching efficiency (ternary DES) after 24 h leaching (each condition was measured once; triplicate values refer to analytical replicates of the same filtrate).

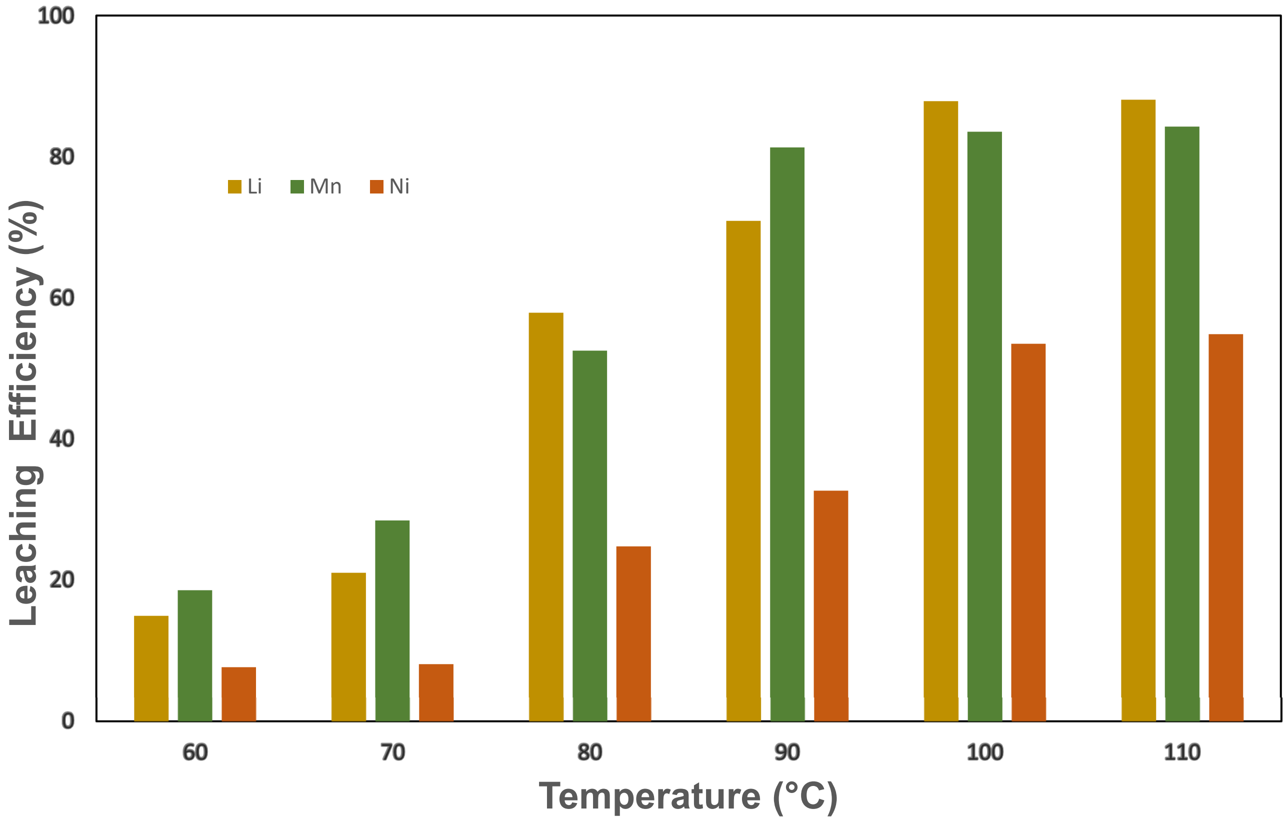

Figure 8. Effect of temperature on leaching efficiency (binary DES) after 24 h leaching (each condition was measured once; triplicate values refer to analytical replicates of the same filtrate).

In contrast, the ternary DES system (Figure 7), modified with 10 wt.% water showed higher performance under experimental conditions at all temperature levels. The addition of water has been shown to significantly reduce the viscosity of DESs, improving ion mobility and enhancing metal dissolution kinetics [48,51,55,57]. At 60 °C, Li, Mn, and Ni showed higher leaching efficiencies (23.5%, 24.5%, and 7.9%, respectively) compared to the binary DES. The efficiencies increased with temperature and reached 98.9%, 98.4%, and 71.4% for Li, Mn, and Ni, respectively, at 110 °C. However, leaching efficiency plateaued beyond 100 °C, indicating that increased temperature no longer yields proportional improvement due to the saturation of metal-DES complexation and changes in solvent structure at elevated temperatures, consistent with observations by [46].

Importantly, the ternary DES achieved >90% recovery for Li and Mn at just 90 °C, whereas the binary DES required 100 °C to reach similar extraction levels. This result underscores the higher reactivity and lower energy demand of the ternary DES, which aligns with recent findings that show aqueous-modified DESs can significantly enhance leaching rates while reducing thermal requirements [58–60].

The values reported in Figure 7 are means of triplicate analytical measurements; as each condition was tested once, the results are presented without error bars and interpreted as observed trends. Overall, these findings demonstrate the superiority of the ternary DES system for metal recovery from spent LIBs, attributable to its lower viscosity, enhanced mass transfer, and improved complexation capacity. Such systems offer a promising low-energy, environmentally friendly alternative to conventional leaching methods.

3.2.2. Effect of Leaching Time on Metal Extraction Efficiency Using Ternary DES

Figure 8 illustrates the effect of leaching time at 100 °C on the extraction efficiency of Li, Mn, and Ni from spent LIB cathode material using the ternary DES system. The results demonstrate a clear time-dependent improvement in metal dissolution, with substantial increases observed as the reaction time progressed from 2 to 24 h.

At the initial stage (2 h), the leaching efficiencies were relatively low, with Li, Mn, and Ni reaching only 29.3%, 3.4%, and 2.0%, respectively. This suggests that the dissolution of active cathode components requires an initial activation period, during which DES components penetrate the solid matrix and begin breaking down the metal-ligand bonds [34,40].

With increasing leaching duration, metal extraction efficiency showed a steady enhancement. After 12 h, Li, Mn, and Ni reached 53.7%, 24.5%, and 12.0%, respectively, indicating that prolonged contact time significantly facilitates the diffusion and solubilization of metal ions into the DES phase.

A substantial improvement was observed after 18 h, where Li and Mn leaching efficiencies reached 87.9% and 42.5%, while Ni extraction remained comparatively lower at 33.1%, likely due to the stronger interaction of Ni within the cathode material lattice. This trend aligns with previous studies reporting that lithium is more readily leached due to its higher mobility and weaker bonding in layered oxide structures, while Ni shows stronger bonding within the crystal lattice, making it less accessible under similar conditions [57,61]. The moderate recovery of Mn is consistent with its intermediate bonding strength and partial reduction during leaching processes. These observations suggest that extended leaching time favors the dissolution of loosely bound metals, while more tightly bound elements like Ni may require harsher conditions or stronger complexing agents for higher recovery.

At 24 h, the dissolution process reached its peak, with Li, Mn, and Ni achieving 98.9%, 98.4%, and 71.2% leaching efficiency, respectively. This indicates that near-complete metal recovery is attainable with prolonged leaching, confirming the high capability of ternary DES in facilitating metal dissolution over extended durations.

These findings indicate that shorter reaction times do not yield optimal recovery, whereas extending the leaching duration beyond 18 h markedly improves efficiency, particularly for Li and Mn. The notable increase in Ni dissolution at longer durations underscores the importance of prolonged leaching for enhanced metal recovery; however, the incomplete Ni dissolution (~71%) suggests the presence of an undissolved solid residue likely enriched in Ni. Due to the small experimental scale (50 mg in 5 mL), the recovered residue was insufficient for phase or elemental analysis. Therefore, no further speculation is made regarding its exact composition.

3.2.3. Visual Indicators of Leaching Efficiency

The color change of the deep eutectic solvent (ternary DES) solution serves as a qualitative marker of metal dissolution, providing visual confirmation of leaching efficiency under varying experimental conditions. As shown in Figure 9, higher temperatures (a) and longer reaction times (b) result in progressively darker solutions, indicating increased dissolution of metal ions into the solvent. This phenomenon aligns with quantitative leaching results, demonstrating that elevated temperatures and extended durations enhance the extraction of lithium and manganese, while nickel exhibits relatively lower solubility under the same conditions. The correlation between color intensity and metal dissolution underscores the potential of DES-based leaching as an efficient and environmentally friendly approach for LIB recycling.

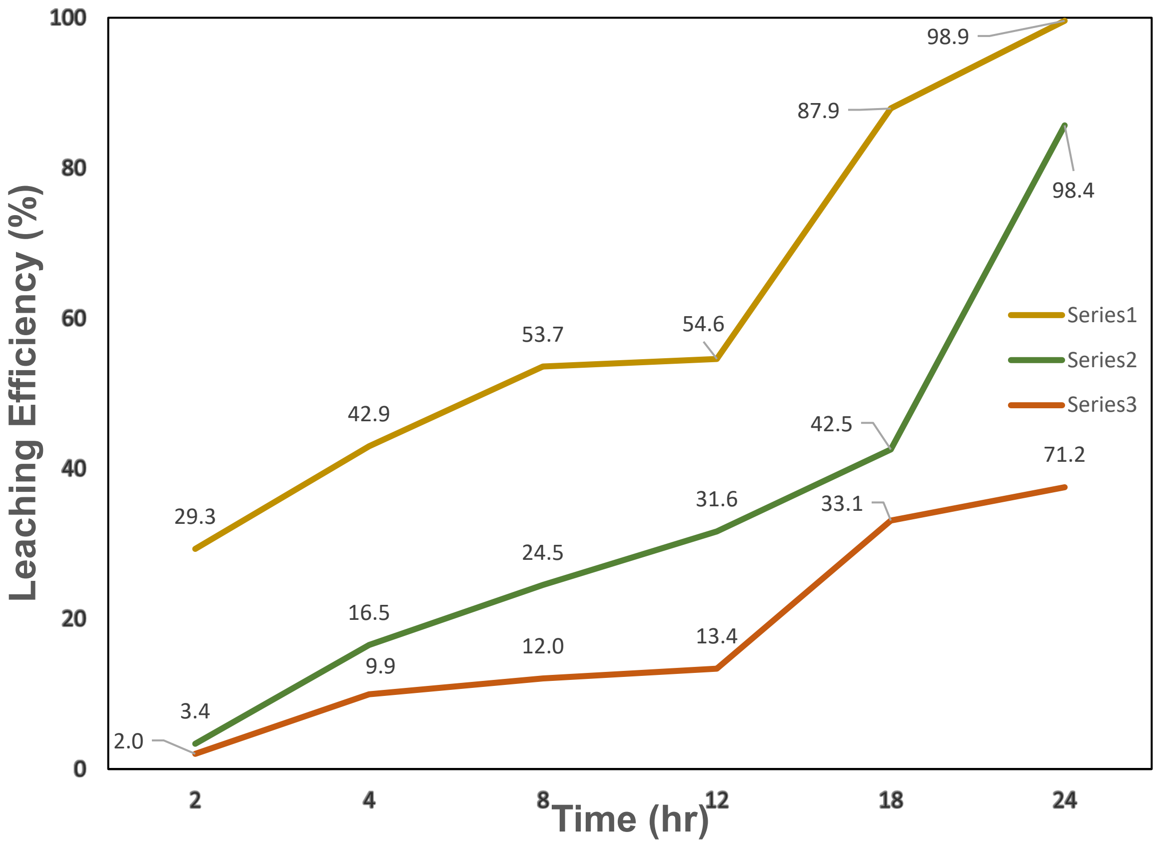

Figure 9. Effect of time on leaching efficiency (ternary DES).

The differences in liquid volume observed in Figure 10b are due to aliquot withdrawal and subsequent dilution for AAS analysis; all leaching efficiencies were calculated based on an initial DES volume of 5.0 mL, and reported concentrations were corrected for the applied dilution factors. In the ChCl–D-glucose–H_2O DES, Li dissolves via rapid de-intercalation and solvation of Li^+ without a redox step [1]. Surface Mn (III/IV) is reduced to Mn (II) by glucose and subsequently stabilized through chloride/oxygen coordination [1]. Ni dissolution is ligand-promoted but proceeds more slowly, consistent with its stronger crystal-field stabilization and M–O bonding within the spinel lattice [62]. Overall, the observed selectivity reflects coordination-environment control in the DES, favoring Li and Mn over Ni under the present conditions [62].

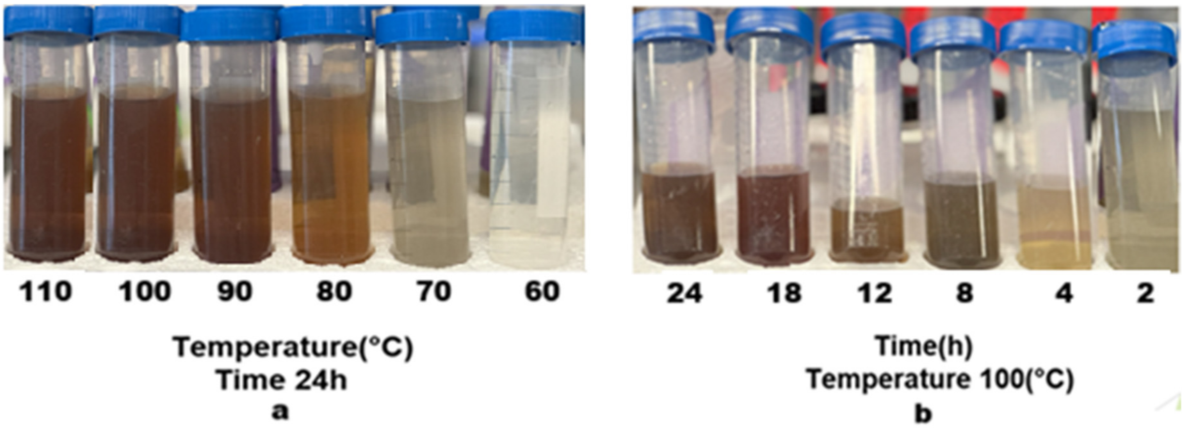

Figure 10. (**a**) Change in color of leaching solution for different temperatures over 24 h. (**b**) Change in color of leaching solution for different times at 100 °C.

4. Conclusions

This study successfully introduced and evaluated the performance of deep eutectic solvents (DESs), with a particular focus on a ternary choline chloride–D-glucose–water formulation, for the selective leaching of Li, Mn, and Ni from spent lithium-ion battery cathodes. By examining the effects of temperature and leaching duration, it provides clear evidence that DES-based hydrometallurgical systems can be optimized for high-efficiency, environmentally sustainable metal recovery.

The ternary DES demonstrated markedly superior performance over its binary counterpart, owing to its reduced viscosity, enhanced mass transfer, and improved metal ion solubility. Incorporating 10 wt.% water significantly accelerated leaching kinetics, enabling near-complete extraction of Li (98.9%) and Mn (98.4%) under optimized conditions, while Ni reached a recovery of 71.7% despite its stronger lattice binding. Efficiency gains plateaued above 100 °C, indicating an optimal temperature threshold, and time-dependent experiments showed that the most substantial improvements occurred within the first 18–24 h. The observed correlation between solution color intensity and metal dissolution further suggests a practical visual indicator for leaching progress.

From a broader perspective, these results confirm the potential of water-enhanced DES systems as a low-energy, non-toxic, and biodegradable alternative to conventional acid-based leaching methods, eliminating the need for strong acids and oxidants. Their tunable coordination environment offers opportunities to selectively target different metals, supporting more sustainable battery recycling pathways. Future studies could focus on tailoring DES compositions to further enhance Ni dissolution, exploring synergistic effects with other green additives, and assessing solvent recyclability and regeneration. Process scale-up with independent replicates and robust statistical analysis will help establish industrial applicability, while economic and life-cycle assessments can guide commercial adoption. By building on the promising outcomes of this work, continued research can accelerate the transition of DES-based recycling into practical, scalable solutions that advance the circular economy for lithium-ion batteries.

Author Contributions: Conceptualization, J.H. and K.Z.; Methodology, J.G. and Z.C.; Formal analysis, G.Z.; Writing—original draft, J.G.; Writing—review & editing, G.Z., J.H., K.Z., S.D., A.A.D., X.W., F.H., C.N.M., C.A. and A.A.R.; Supervision, Z.C.; Funding acquisition, Z.C. All authors have read and agreed to the published version of the manuscript.

Funding: This research was financially supported by the Volt-Age Seed Grant at Concordia University.

Data Availability Statement: The original contributions presented in this study are included in the article. Further inquiries can be directed to the corresponding author.

Conflicts of Interest: The authors declare no conflicts of interest.

References

1. Tran, M.K.; Rodrigues, M.-T.F.F.; Kato, K.; Babu, G.; Ajayan, P.M. Deep eutectic solvents for cathode recycling of Li-ion batteries. *Nat. Energy* **2019**, *4*, 339–345. [CrossRef]
2. Garole, D.J.; Hossain, R.; Garole, V.J.; Sahajwalla, V.; Nerkar, J.; Dubal, D.P. Recycle, Recover and Repurpose Strategy of Spent Li-ion Batteries and Catalysts: Current Status and Future Opportunities. *ChemSusChem* **2020**, *13*, 3079–3100. [CrossRef] [PubMed]
3. Li, P.; Luo, S.; Zhang, L.; Liu, Q.; Wang, Y.; Lin, Y.; Xu, C.; Guo, J.; Cheali, P.; Xia, X. Progress, challenges, and prospects of spent lithium-ion batteries recycling: A review. *J. Energy Chem.* **2024**, *89*, 144–171. [CrossRef]
4. Yu, H.; Yang, H.; Chen, K.; Yang, L.; Huang, M.; Wang, Z.; Lv, H.; Xu, C.; Chen, L.; Luo, X. Non–closed–loop recycling strategies for spent lithium–ion batteries: Current status and future prospects. *Energy Storage Mater.* **2024**, *67*, 103288. [CrossRef]
5. Milian, Y.E.; Jamett, N.; Cruz, C.; Herrera-León, S.; Chacana-Olivares, J. A comprehensive review of emerging technologies for recycling spent lithium-ion batteries. *Sci. Total Environ.* **2024**, *910*, 168543. [CrossRef] [PubMed]
6. Castro, F.D.; Cutaia, L.; Vaccari, M. End-of-life automotive lithium-ion batteries (LIBs) in Brazil: Prediction of flows and revenues by 2030. *Resour. Conserv. Recycl.* **2021**, *169*, 105522. [CrossRef]
7. Zhang, K.; Liang, H.; Zhong, X.; Cao, H.; Wang, R.; Liu, Z. Recovery of metals from sulfate leach solutions of spent ternary lithium-ion batteries by precipitation with phosphate and solvent extraction with P507. *Hydrometallurgy* **2022**, *210*, 105861. [CrossRef]
8. Makuza, B.; Tian, Q.; Guo, X.; Chattopadhyay, K.; Yu, D. Pyrometallurgical options for recycling spent lithium-ion batteries: A comprehensive review. *J. Power Sources* **2021**, *491*, 229622. [CrossRef]
9. Liang, J.; Chen, R.; Gu, J.-N.; Li, J.; Xue, Y.; Shi, F.; Huang, B.; Guo, M.; Jia, J.; Li, K.; et al. Sustainable recycling of spent ternary lithium-ion batteries via an environmentally friendly process: Selective recovery of lithium and non-hazardous upcycling of residue. *Chem. Eng. J.* **2024**, *481*, 148516. [CrossRef]
10. Rehman, S.; Al-Greer, M.; Burn, A.S.; Short, M.; Cui, X. High-Volume Battery Recycling: Technical Review of Challenges and Future Directions. *Batteries* **2025**, *11*, 94. [CrossRef]
11. Lombardo, G.; Ebin, B.; St. Foreman, M.R.J.; Steenari, B.-M.; Petranikova, M. Chemical Transformations in Li-Ion Battery Electrode Materials by Carbothermic Reduction. *ACS Sustain. Chem. Eng.* **2019**, *7*, 13668–13679. [CrossRef]
12. Sethurajan, M.; Gaydardzhiev, S. Bioprocessing of spent lithium-ion batteries for critical metals recovery—A review. *Resour. Conserv. Recycl.* **2021**, *165*, 105225. [CrossRef]
13. Xiao, J.; Niu, B.; Song, Q.; Zhan, L.; Xu, Z. Novel targetedly extracting lithium: An environmental-friendly controlled chlorinating technology and mechanism of spent lithium-ion batteries recovery. *J. Hazard. Mater.* **2021**, *404*, 123947. [CrossRef]
14. Fan, Y.; Kong, Y.; Jiang, P.; Zhang, G.; Cong, J.; Shi, X.; Liu, Y.; Zhang, P.; Zhang, R.; Huang, Y. Development and challenges of deep eutectic solvents for cathode recycling of end-of-life lithium-ion batteries. *Chem. Eng. J.* **2023**, *463*, 142278. [CrossRef]
15. Tarascon, J.-M.; Armand, M. Issues and challenges facing rechargeable lithium batteries. *Nature* **2001**, *414*, 359–367. [CrossRef]
16. Goodenough, J.B.; Park, K.-S. The Li-Ion Rechargeable Battery: A Perspective. *J. Am. Chem. Soc.* **2013**, *135*, 1167–1176. [CrossRef]
17. Ebrahimi, E.; Kordloo, M.; Khodadadmahmoudi, G.; Rezaei, A.; Ganjali, M.; Azimi, G. Solvometallurgical recycling of spent LiNixCoyMnzO2 (NCM) cathode material using ternary choline chloride-ethylene glycol-p-toluenesulfonic acid deep eutectic solvent. *Hydrometallurgy* **2023**, *222*, 106184. [CrossRef]
18. Khan, S.A.; Ali, S.; Saeed, K.; Usman, M.; Khan, I. Advanced cathode materials and efficient electrolytes for rechargeable batteries: Practical challenges and future perspectives. *J. Mater. Chem. A* **2019**, *7*, 10159–10173. [CrossRef]
19. He, M.; Rohani, S.; Teng, L.; Gao, Y.; Jin, X.; Zhang, X.; Liu, Q.; Liu, W. Thermochemically driven layer structure collapse via sulfate roasting toward the selective extraction of lithium and cobalt from spent LiCoO2 batteries. *J. Power Sources* **2023**, *572*, 233094. [CrossRef]
20. Rensmo, A.; Savvidou, E.K.; Cousins, I.T.; Hu, X.; Schellenberger, S.; Benskin, J.P. Lithium-ion battery recycling: A source of per- and polyfluoroalkyl substances (PFAS) to the environment? *Environ. Sci. Process. Lmpacts* **2023**, *25*, 1015–1030. [CrossRef]

21. Gaines, L. Lithium-ion battery recycling processes: Research towards a sustainable course. *Sustain. Mater. Technol.* **2018**, *17*, e00068. [CrossRef]
22. He, M.; Jin, X.; Zhang, X.; Duan, X.; Zhang, P.; Teng, L.; Liu, Q.; Liu, W. Combined pyro-hydrometallurgical technology for recovering valuable metal elements from spent lithium-ion batteries: A review of recent developments. *Green Chem.* **2023**, *25*, 6561–6580. [CrossRef]
23. Chen, Z.; Yildizbasi, A.; Wang, Y.; Sarkis, J. Safety Concerns for the Management of End-of-Life Lithium-Ion Batteries. *Glob. Chall.* **2022**, *6*, 202200049. [CrossRef]
24. Cornelio, A.; Zanoletti, A.; Bontempi, E. Recent progress in pyrometallurgy for the recovery of spent lithium-ion batteries: A review of state-of-the-art developments. *Curr. Opin. Green Sustain. Chem.* **2024**, *46*, 100881. [CrossRef]
25. Reinhart, L.; Vrucak, D.; Woeste, R.; Lucas, H.; Rombach, E.; Friedrich, B.; Letmathe, P. Pyrometallurgical recycling of different lithium-ion battery cell systems: Economic and technical analysis. *J. Clean. Prod.* **2023**, *416*, 137834. [CrossRef]
26. Dalini, E.A.; Karimi, G.; Zandevakili, S.; Goodarzi, M. A Review on Environmental, Economic and Hydrometallurgical Processes of Recycling Spent Lithium-ion Batteries. *Miner. Process. Extr. Metall. Rev.* **2020**, *42*, 451–472. [CrossRef]
27. Liu, C.; Yu, J.; Hu, J.; Xu, J.; Yu, A.; Liu, T.; Wang, Z.; Luo, X.; Deng, C.; Luo, F.; et al. Ultra-low viscosity betaine hydrochloride-formic acid deep eutectic solvent for leaching critical metals from spent NCM lithium-ion batteries. *J. Environ. Chem. Eng.* **2024**, *12*, 112586. [CrossRef]
28. Guimarães, L.; Junior, A.B.; Espinosa, D. Sulfuric acid leaching of metals from waste Li-ion batteries without using reducing agent. *Miner. Eng.* **2022**, *183*, 107597. [CrossRef]
29. Rouquette, L.M.; Petranikova, M.; Vieceli, N. Complete and selective recovery of lithium from EV lithium-ion batteries: Modeling and optimization using oxalic acid as a leaching agent. *Sep. Purif. Technol.* **2023**, *320*, 124143. [CrossRef]
30. Ren, L.; Liu, B.; Bao, S.; Ding, W.; Zhang, Y.; Hou, X.; Lin, C.; Chen, B. Recovery of Li, Ni, Co and Mn from spent lithium-ion batteries assisted by organic acids: Process optimization and leaching mechanism. *Int. J. Miner. Metall. Mater.* **2024**, *31*, 518–530. [CrossRef]
31. Ji, H.; Wang, J.; Ma, J.; Cheng, H.-M.; Zhou, G. Fundamentals, status and challenges of direct recycling technologies for lithium-ion batteries. *Chem. Soc. Rev.* **2023**, *52*, 8194–8244. [CrossRef] [PubMed]
32. Wang, M.; Liu, K.; Yu, J.; Zhang, Q.; Zhang, Y.; Valix, M.; Tsang, D.C. Challenges in Recycling Spent Lithium-Ion Batteries: Spotlight on Polyvinylidene Fluoride Removal. *Glob. Chall.* **2023**, *7*, 2200237. [CrossRef] [PubMed]
33. Abbott, A.P.; Boothby, D.; Capper, G.; Davies, D.L.; Rasheed, R.K. Deep Eutectic Solvents formed between choline chloride and carboxylic acids: Versatile alternatives to ionic liquids. *J. Am. Chem. Soc.* **2004**, *126*, 9142–9147. [CrossRef]
34. Peeters, N.; Binnemans, K.; Riaño, S. Solvometallurgical recovery of cobalt from lithium-ion battery cathode materials using deep-eutectic solvents. *Green Chem.* **2020**, *22*, 4210–4221. [CrossRef]
35. Yuan, Z.; Liu, H.; Yong, W.F.; She, Q.; Esteban, J. Status and advances of deep eutectic solvents for metal separation and recovery. *Green Chem.* **2022**, *24*, 1895–1929. [CrossRef]
36. Abbott, A.P.; Capper, G.; Davies, D.L.; McKenzie, K.J.; Obi, S.U. Solubility of metal oxides in deep eutectic solvents based on choline chloride. *J. Chem. Eng. Data* **2006**, *51*, 1280–1282. [CrossRef]
37. Wang, S.; Tian, Y.; Zhang, X.; Yang, B.; Wang, F.; Xu, B.; Liang, D.; Wang, L. A Review of Processes and Technologies for the Recycling of Spent Lithium-ion Batteries. *IOP Conf. Ser. Mater. Sci. Eng.* **2020**, *782*, 022025. [CrossRef]
38. Zhou, M.; Shen, J.; Duan, Y.; Zuo, Y.; Xing, Z.; Liu, R. The Le Chatelier's principle enables closed loop regenerating ternary cathode materials for spent lithium-ion batteries. *Energy Storage Mater.* **2024**, *67*, 103250. [CrossRef]
39. Jin, X.; Zhang, P.; Teng, L.; Rohani, S.; He, M.; Meng, F.; Liu, Q.; Liu, W. Acid-free extraction of valuable metal elements from spent lithium-ion batteries using waste copperas. *Waste Manag.* **2023**, *165*, 189–198. [CrossRef]
40. Wang, S.; Zhang, Z.; Lu, Z.; Xu, Z. A novel method for screening deep eutectic solvent to recycle the cathode of Li-ion batteries. *Green Chem.* **2020**, *22*, 4473–4482. [CrossRef]
41. Zhu, A.; Bian, X.; Han, W.; Cao, D.; Wen, Y.; Zhu, K.; Wang, S. The application of deep eutectic solvents in lithium-ion battery recycling: A comprehensive review. *Resour. Conserv. Recycl.* **2023**, *188*, 106690. [CrossRef]
42. Srivastava, V.; Rantala, V.; Mehdipour, P.; Kauppinen, T.; Tuomikoski, S.; Heponiemi, A.; Runtti, H.; Tynjälä, P.; Dos Reis, G.S.; Lassi, U. A comprehensive review of the reclamation of resources from spent lithium-ion batteries. *Chem. Eng. J.* **2023**, *474*, 145822. [CrossRef]
43. Schiavi, P.G.; Altimari, P.; Branchi, M.; Zanoni, R.; Simonetti, G.; Navarra, M.A.; Pagnanelli, F. Selective recovery of cobalt from mixed lithium-ion battery wastes using deep eutectic solvent. *Chem. Eng. J.* **2021**, *417*, 129249. [CrossRef]
44. Su, R.; Tang, S.; Zhang, M.; Guo, M. Strategies for overcoming challenges in using deep eutectic solvents for the selective extraction of valuable metals from spent lithium-ion batteries: A review. *J. Environ. Chem. Eng.* **2024**, *12*, 113200. [CrossRef]
45. Dorella, G.; Mansur, M.B. A study of the separation of cobalt from spent Li-ion battery residues. *J. Power Sources* **2007**, *170*, 210–215. [CrossRef]

46. Behnajady, B.; Seyf, J.Y.; Karimi, S.; Moradi, M.; Sohrabi, M. Molecular dynamic (MD) simulation and density function theory (DFT) calculation relevant to green leaching of metals from spent lithium-ion battery cathode materials using glucose-based deep eutectic solvent (DES). *Hydrometallurgy* **2024**, *223*, 106223. [CrossRef]
47. Golmohammadzadeh, R.; Rashchi, F.; Vahidi, E. Recovery of lithium and cobalt from spent lithium-ion batteries using organic acids: Process optimization and kinetic aspects. *Waste Manag.* **2017**, *64*, 244–254. [CrossRef] [PubMed]
48. Seyf, J.Y.; Zarei, F. Density, Viscosity, and Refractive Index of a Choline Chloride + d -(-)-Fructose Deep Eutectic Solvent + Water Mixture at Different Temperatures: An Experimental Study and Thermodynamic Modeling. *J. Chem. Eng. Data* **2022**, *67*, 3007–3021. [CrossRef]
49. Smith, E.L.; Abbott, A.P.; Ryder, K.S. Deep Eutectic Solvents (DESs) and Their Applications. *Chem. Rev.* **2014**, *114*, 11060–11082. [CrossRef]
50. Gabriele, F.; Chiarini, M.; Germani, R.; Tiecco, M.; Spreti, N. Effect of water addition on choline chloride/glycol deep eutectic solvents: Characterization of their structural and physicochemical properties. *J. Mol. Liq.* **2019**, *291*, 11301. [CrossRef]
51. Aravena, P.; Cea-Klapp, E.; Gajardo-Parra, N.F.; Held, C.; Garrido, J.M.; Canales, R.I. Effect of water and hydrogen bond acceptor on the density and viscosity of glycol-based eutectic solvents. *J. Mol. Liq.* **2023**, *389*, 122856. [CrossRef]
52. Kivelä, H.; Salomäki, M.; Vainikka, P.; Mäkilä, E.; Poletti, F.; Ruggeri, S.; Terzi, F.; Lukkari, J. Effect of Water on a Hydrophobic Deep Eutectic Solvent. *J. Phys. Chem. B* **2022**, *126*, 513–527. [CrossRef]
53. Meredith, L.; Elbourne, A.; Greaves, T.L.; Bryant, G.; Bryant, S.J. Physico-chemical characterisation of glycerol- and ethylene glycol-based deep eutectic solvents. *Mol. Liq.* **2024**, *394*, 123777. [CrossRef]
54. Rozas, S.; Benito, C.; Alcalde, R.; Atilhan, M.; Aparicio, S. Insights on the water effect on deep eutectic solvents properties and structuring: The archetypical case of choline chloride + ethylene glycol. *J. Mol. Liq.* **2021**, *344*, 117717. [CrossRef]
55. Peng, D.; Yu, Z.; Alhadid, A.; Minceva, M. Modeling the Viscosity of ChCl-Based Deep Eutectic Solvents and Their Mixtures with Water. *Ind. Eng. Chem. Res.* **2024**, *63*, 1623–1633. [CrossRef]
56. Ma, Y.; Yang, Y.; Li, T.; Hussain, S.; Zhu, M. Deep eutectic solvents as an emerging green platform for the synthesis of functional materials. *Green Chem.* **2024**, *26*, 3627–3669. [CrossRef]
57. Chen, Y.; Zhang, F.; Yang, C.; Ju, X.; Zhang, Z.; Liu, Z.; Yang, M. Efficient and Selective Dissolution of Li from Lithium-Ion Battery LiFePO4 Cathode by Natural Deep Eutectic Solvents. *Energy Fuels* **2024**, *38*, 5391–5396. [CrossRef]
58. Wang, J.; Lyu, Y.; Zeng, R.; Zhang, S.; Davey, K.; Mao, J.; Guo, Z. Green recycling of spent Li-ion battery cathodes via deep-eutectic solvents. *Energy Environ. Sci.* **2023**, *17*, 867–884. [CrossRef]
59. Padwal, C.; Pham, H.D.; Jadhav, S.; Do, T.T.; Nerkar, J.; Hoang, L.T.M.; Nanjundan, A.K.; Mundree, S.G.; Dubal, D.P. Deep Eutectic Solvents: Green Approach for Cathode Recycling of Li-Ion Batteries. *Adv. Energy Sustain. Res.* **2022**, *3*, 2100133. [CrossRef]
60. Shaibuna, M.; Theresa, L.V.; Sreekumar, K. Neoteric deep eutectic solvents: History, recent developments, and catalytic applications. *Soft Matter* **2022**, *18*, 2695–2721. [CrossRef]
61. Zhang, G.; Yuan, X.; He, Y.; Wang, H.; Zhang, T.; Xie, W. Recent advances in pretreating technology for recycling valuable metals from spent lithium-ion batteries. *J. Hazard. Mater.* **2021**, *406*, 124332. [CrossRef] [PubMed]
62. Chang, X.; Fan, M.; Gu, C.; He, W.; Meng, Q.; Wan, L.; Guo, Y. Selective extraction of transition metals from spent $LiNi_xCo_\gamma Mn_{1-x-\gamma}O_2$ cathode via regulation of coordination environment. *Angew. Chem. Int. Ed.* **2022**, *61*, e202202558. [CrossRef] [PubMed]